### Title

Aqueous geochemistry at gigapascal pressures: NMR spectroscopy of fluoroborate solutions




### Authors

Ochoa, Gerardo
Pilgrim, Corey D
Kerr, Julia
et al.



### Publication Date

2019

### DOI

10.1016/j.gca.2018.09.033

Peer reviewed

Available online at www.sciencedirect.com

ScienceDirect

Geochimica et Cosmochimica Acta 244 (2019) 173–181

Geochimica et Cosmochimica Acta

www.elsevier.com/locate/gca

# Aqueous geochemistry at gigapascal pressures: NMR spectroscopy of fluoroborate solutions

Gerardo Ochoa [a], Corey D. Pilgrim [a], Julia Kerr [a], Matthew P. Augustine [a] William H. Casey [a,b,*]

[a] Department of Chemistry, University of California, Davis, 1 Shields Ave, Davis, CA 95616, USA
[b] Department of Earth and Planetary Sciences, University of California, Davis, 1 Shields Ave, Davis, CA 95616, USA

Received 27 April 2018; accepted in revised form 29 September 2018; Available online 10 October 2018

**Abstract**

Aqueous geochemistry could be extended considerably if nuclear-magnetic resonance (NMR) methods could be adapted to study solutions at elevated temperatures and pressures. We therefore designed an NMR probe that can be used to study aqueous solutions at gigapascal pressures. Fluoride solutions were chosen for study because $^{19}F$ couples to other nuclei in the solutions ($^{31}P$ and $^{11}B$) in ways that make peak assignments unequivocal. Correspondingly, NMR spectra of $^{19}F$- and $^{11}B$ were collected on aqueous $HBF_4$-$NH_4PF_6$ solutions to pressures up to 2.0 GPa. At pressure, peaks in the $^{19}F$ spectra were clear and assignable to the $BF_4^-$(aq), $F^-$(aq) and $BF_3OH^-$ (aq) ions, and these aqueous complexes varied in signal intensity with pressure and time, for each solution. Peaks in the $^{11}B$ spectra at pressure could be assigned to the $BF_4^-$(aq) and $BF_3OH^-$(aq) species. Additionally, there is a single peak that is assignable to $H_3BO_3^0$(aq) and $B(OH)_4^-$(aq) in rapid-exchange equilibria. These peaks broaden and move with pressure in ways that suggest reversible interconversion of borate and fluoroborate species. The $PF_6^-$ ion was found to provide a suitable $^{19}F$ shift and intensity standard for high-pressure spectra because it was chemically inert. The positions and intensities of the doublet peak also remains constant as a function of pressure and pH. Addition of electrolytes considerably distorts the phase diagram of water such that the stability region of the aqueous solution expands to well beyond the 0.8 GPa freezing pressure of pure water; some fluoroborate solutions remain liquid until almost 2.0 GPa.


*Keywords:* Spectroscopy; NMR; Aqueous solutions; High-pressure; Kinetics

## 1. INTRODUCTION

Geochemists developed models to predict solute speciation and mineral equilibria in aqueous solutions to 1200 °C and 6.0 GPa. These models are a primary geochemical tool for uncovering reaction pathways in the Earth (see Sverjensky et al., 2014; Sverjensky and Huang, 2015). The need for these models is compelling but the conditions are well beyond the limits of conventional NMR spectroscopy. This gap in technology inspired us to design a high-pressure NMR probe that can resolve signals from solute species in aqueous solutions at gigapascal pressures (Pautler et al., 2014; Ochoa et al., 2015, 2016).

The challenges to geochemists of high-pressure NMR on aqueous solutions are considerable. For example, the sample volume must be larger than a few microliters if induction methods of detecting NMR signals are employed; one needs $\sim 10^{20}$ spins in the RF coil. The need for such volumes precludes the facile use of diamond-anvil cells for detecting aqueous solutes as the volumes of the diamond anvils are nanoliters or less (see Meier et al., 2017; Meier, 2018). Another challenge for aqueous solution geochemists

* Corresponding author at: Department of Chemistry, University of California, Davis, 1 Shields Ave, Davis, CA 95616, USA.
*E-mail address:* whcasey@ucdavis.edu (W.H. Casey).

https://doi.org/10.1016/j.gca.2018.09.033
0016-7037/

is the need to identify a new chemical-shift standard for the chemical system that is studied. As pressures increase to a few gigapascals at near-ambient temperatures, the relative permittivity of water, and thus the Brønsted acid-base properties of solutes, changes dramatically. The signals from shift standards commonly change accordingly and thus become useless, or the compound simply decomposes.

In this paper we collect information on aqueous solutes via $^{19}$F- and $^{11}$B NMR spectra at gigapascal pressures. Fluoroborate solutions were chosen not because the ions are common in geochemical fluids, but because the $BF_4^-$(aq) ion has coupled $^{19}$F- and $^{11}$B NMR spectra ($J_{FB} = \sim 15$ Hz) and because we could identify a chemical-shift standard, the $PF_6^-$(aq) ion, which has useful coupling between $^{19}$F and $^{31}$P and is unreactive. The constant couplings allow the speciation to be interpreted unequivocally because the peak positions do not move with pressure or pH. The probe design differs significantly from that described by Pautler et al (2014) and Ochoa et al. (2016) in that the aqueous solution is also used as the pressure-transmission fluid (see Augustine et al., 2017); thus the sample volume is increased from ~15 μL to ~0.4 mL. The pressures reached (~2.0 GPa) corresponds to pressures of the upper mantle, albeit at near-ambient temperatures.

## 2. EXPERIMENTAL METHODS

### 2.1. Solution chemistry

All solutions were prepared from 18 MΩ water. For determining properties of the shift standard, two 1.0 M $NH_4PF_6$ solutions were created by weighing the appropriate amount of reagent-grade $NH_4PF_6$ into a volume of $H_2O$ and then titrating to pH = 3.5 and pH = 10.0 with NaOH. Fluoroboric acid/ammonium hexafluorophosphate solutions were created by weighing the appropriate amount of reagent-grade $NH_4PF_6$ into a prepared solution of $HBF_4$ in $H_2O$.

The pH of the fluoroborate solutions varies both with time and pressure, due to the slow hydrolysis of $BF_4^-$(aq) to fluoride and boric acid and because of the changing Brønsted acid-base chemistry with pressure. Therefore we denote as pH° the pH values initially measured at ambient pressure. The pH was adjusted with the addition of solid NaOH or aqueous $NH_4OH$. Four separate solutions were used in this study: (1) 2.28 M $HBF_4$, 0.83 M $NH_4PF_6$, 2.68 M NaOH, pH° = 13.0; (2) 0.57 M $HBF_4$, 0.22 M $NH_4PF_6$, 0.83 M $NH_4OH$, pH° = 8.1; (3) 0.59 M $HBF_4$, 0.22 M $NH_4PF_6$, 0.69 M $NH_4OH$, pH° = 5.1; (4) 0.60 M $HBF_4$, 0.22 M $NH_4PF_6$, 0.60 M $NH_4OH$, pH° = 3.3. Solution **1** was intentionally saturated with the mineral Villiaumite [NaF(s)] before running the pressure experiments and the composition is therefore *as analyzed*, not *as prepared*. The identity of the precipitate was confirmed as Villiaumite, and not Ferrucite [$NaBF_4$(s)], via powder X-ray diffraction. The pH measurements were made with a combination glass electrode that was calibrated using standard 0.05 M buffers.

The viscosities were measured at ambient conditions using a kinematic viscometer. The relative viscosities were then estimated by dividing by the viscosity of distilled water at the same temperature. These relative viscosities are as follows: water = 1.000 ± 0.004; **(1)** 1.090 ± 0.005, **(2)** 1.030 ± 0.005, **(3)** 0.999 ± 0.004, and **(4)** 1.006 ± 0.005, with the uncertainties corresponding to one estimated standard error of the mean.

### 2.2. $^{19}$F and $^{11}$B NMR Spectroscopy

The design of the high-pressure NMR probe is described in earlier papers (Pautler et al., 2014; Augustine et al., 2017) and will not be discussed at length here. Internal pressure was estimated from gauge pressure on a laboratory hydraulic press using an external calibration curve based upon fluorescence of a ruby coupled to a fiberoptic cable (Fig. S-1). Uncertainties in pressure are estimated to be ±0.1 GPa (one estimated standard deviation). Metal parts of the microcoil geometry were protected from corrosion by the sample solution by coating them with a thin layer of epoxy and latex.

The $^{19}$F spectra at pressure were collected at 42.23 MHz on an Aspect Imaging M2™ compact MRI instrument built around a permanent 1.05 T magnet that was interfaced to a Tecmag™ Redstone spectrometer. Shimming was performed on the single $^1$H peak in the solvent water by increasing the radio frequency (RF) to 44.89 MHz. Here an automated Matlab™ code controlled the Redstone pulse programmer ($^1$H pulse parameters: π/2 pulse = 18 μs, relaxation delay = 3 s). An RF-pulse tip angle of 31.2° (4.1 μs) with a relaxation delay of 500 ms was used for all $^{19}$F spectra (see Ernst and Anderson, 1966). Data analysis of $^{19}$F spectra collected at pressure was accomplished by signal-averaging 200 two-dimensional (2D) scans over a 15-h period; each 2D scan contained 500 individual scans. This 2-D method was necessary to compensate for drift of the magnetic field. Compensation was accomplished using a Matlab™ code that adjusted the spectra using the $PF_6^-$(aq) signal as a standard. Additional high-resolution, ambient $^{19}$F spectra for all solutions were collected at 470.54 MHz using an 11.7 T superconducting magnet interfaced to a Bruker DRX spectrometer.

The $^{11}$B NMR spectra of solutions **1**–**3** were acquired at 74.41 MHz using at 6.95 T Oxford Instruments 78-mm-bore superconducting magnet that was interfaced to a Tecmag Orion™ spectrometer. A single-pulse acquisition was used, with π/2 pulse of 29 μs and a relaxation delay of 200 ms. Additional $^{11}$B NMR spectra on solution **2** were collected from ambient pressure to 1.3 GPa at 42.99 MHz using a Bruker spectrometer that was built around a 9.398 T superconducting magnet. Shimming for these experiments were accomplished by changing the RF to 61.42 MHz in order to detect the $^2$H signal of $D_2O$ in the solvent of solution **2** at each pressure and shimming until the peak width was approximately 70 Hz at full-width-at-half-maximum (Supplemental Information). NMR parameters for the $^2$H shimming experiments were a π/2 pulse length of 10 μs, and a relaxation delay of 250 μs. The high-pressure $^{11}$B NMR spectra were collected with a π/2 pulse length of 10 μs, relaxation delay of 500 μs, and 1600 scans.

All raw data at ambient pressures from the Bruker probe were processed via simple direct Fourier transformation in the Mestrenova© software (the 'FT' utility) and corrected using the conventional power-series phase correction within

that software. Data for the high-pressure probe from the TechMag© spectrometer were Fourier-transformed and stacked using in-house data-processing algorithms written for MatLab; these are included in the Supplemental Information. The TNTFileread.m program takes the raw spectral FID, corrects for magnetic-field drift, Fourier-transforms it and corrects the data for phase. No line broadening or zero-filling corrections were executed; no data were rejected.

## 3. RESULTS

### 3.1. $^{19}$F NMR shift standard

The first step is to reference peak positions. This means that an internal standard for high-pressure experiments must be identified that is both chemically inert and that presents a clear NMR signal that is impervious to changes in pressure. Ideally, such a shift standard not only allows us to reference peak positions as a function of pressure but can also be used as a constant-intensity standard for gauging changes in other signals. The $PF_6^-$(aq) ion was investigated as a standard because it is chemically inert, does not coordinate to metals and the NMR behavior is well characterized (Baghurst et al., 1989; Kubas et al., 2007; Amaya et al., 2010; Arunachalam et al., 2010). The $NH_4PF_6$ salt is highly soluble in water and the $^{19}$F NMR signal of the $PF_6^-$ ion yields two signals (Fig. 1). This doublet is due to the $^{19}$F-$^{31}$P coupling. The $^{19}$F-$^{31}$P J-coupling was measured to be 742.7 Hz at ambient pressure and 742.2 Hz at a pressure of 1.3 GPa, which is constant to within our experimental ability to resolve chemical shifts at pressure, which is 1.5–2 ppm (Augustine et al., 2017). Upon lowering the pH of the solution to 3.5, the measured J-coupling remained constant at 742.2 Hz over the entire pressure range from ambient to 1.3 GPa, but the experimental solution froze at $P > 1.3$ GPa. In all cases, returning to ambient pressure after freezing yields the original signal (Fig. 1), indicating that there were no irreversible changes upon freezing, and neither the peak midpoint, nor the separations (J-coupling), were found to change with pressure or pH (Fig. 1).

### 3.2. $^{19}$F NMR of fluoroborate species

The hydrolysis of fluoroboric acid, $HBF_4$:

$$H_2O(l) + BF_4^-(aq) = F^-(aq) + BF_3(OH)^-(aq) + H^+(aq) \quad (1)$$

has been studied before (Wamser, 1948; Freire et al., 2010) at ambient conditions and the reactants and products can be seen in $^{19}$F and $^{11}$B NMR spectra. At ambient conditions the $BF_4^-$(aq) ion persists for days to weeks, which is long enough for these experiments since a typical pressure series is complete six days after initial solution preparation. Equilibrium speciation is reported in the Supplemental Information (see also Mesmer et al., 1973) and all of the expected hydrolysis products can be identified at ambient pressures.

A key point about Eq. (1) is that bulk waters are on the left-hand-side of the equilibrium. Thus, the reaction products will be favored as pressure is elevated because bulk waters are eliminated and packed into the coordination shell of B(III). Stated differently, the volume change for reaction (1) will be negative even though the coordination numbers of both boron and fluoride are conserved by the reaction.

The $^{19}$F spectra for solutions **1**–**4** at ambient conditions (Fig. 2) are fully consistent with literature results (Kuhlmann and Grant, 1964). The 1:1:1:1 splitting near −141 ppm in the $^{19}$F spectra ($J_{FB} \sim 14.5$ Hz) is consistent with coupling to $^{11}$B, but such $^{19}$F-$^{11}$B coupling is not observed in the mineral-saturated solution, possibly because the moderately increased solution viscosity leads to degradation of the signal resolution by slowing the molecular tumbling rates, or because of extensive ion pairing, or both.

The high-pressure probe has insufficient resolution to detect $^{19}$F-$^{11}$B splittings that are apparent in Fig. 2, but two peaks near −150 ppm in the $^{19}$F spectra are clear and assignable to the $BF_4^-$(aq) and the $BF_3OH^-$(aq) ions (Fig. 3), with the largest intensity corresponding to the $BF_4^-$(aq) ion and the $BF_3OH^-$(aq) species appearing as a sharp peak on the downfield shoulder (to the left). The higher hydrolysis complexes, $[BF_2(OH)_2]^-$(aq) and $[BF(OH)_3]^-$(aq) are present at very low intensities, but are labeled in the figure. Those signals are below the detection limit in the high-pressure NMR probe. The intensities of these two peaks in the $^{19}$F NMR spectra in most cases change slightly in relative intensity with pressure and with time, with two profound exceptions.

First, experiments with solution **2** (at pH° = 8.1) showed that the relative intensities of the peaks assigned to the $BF_4^-$(aq) and $BF_3OH^-$(aq) ions could apparently be reversed over the pressure range 1.3–1.6 GPa. The relative intensities return as pressure is relieved. Pressurization of solution **2** produces the anticipated relative concentrations of $BF_4^-$(aq) and the hydrolysis species $BF_3OH^-$(aq) at 1.3 GPa (Fig. 3A), but at 1.6 GPa the formation of $BF_3OH^-$(aq) is more prominent than the $BF_4^-$(aq) (Fig. 3B). This result indicates that hydrolysis of the fluoroborate ion can be enhanced by pressure, as expected from reaction (1), above, and the clear shift in peak positions indicates the reversible interconversion of $BF_3OH^-$(aq) and $BF_4^-$(aq). The equilibrium speciation at ambient conditions (Supplemental Information) indicates the coexistence of these two species, $BF_3OH^-$(aq) and $BF_4^-$(aq) in acidic solutions, but not at the pH° of solution **2**.

The resonance from the free $F^-$(aq) ion that is released by hydrolysis is detectable both in the $^{19}$F spectra at ambient pressures using a high-resolution commercial probe, and in the high-pressure spectra (Fig. 4). Sets of spectra over a range of pH° conditions are compiled in the Supplemental Information. As expected, the signal assignable to the hydrolysis species $BF_3OH^-$(aq) also becomes more prominent in solutions where the pH has been lowered to 5.1 and 3.3.

Secondly, in some solutions, the signal intensity for the $BF_4^-$(aq) species declines or disappears as the pressure is

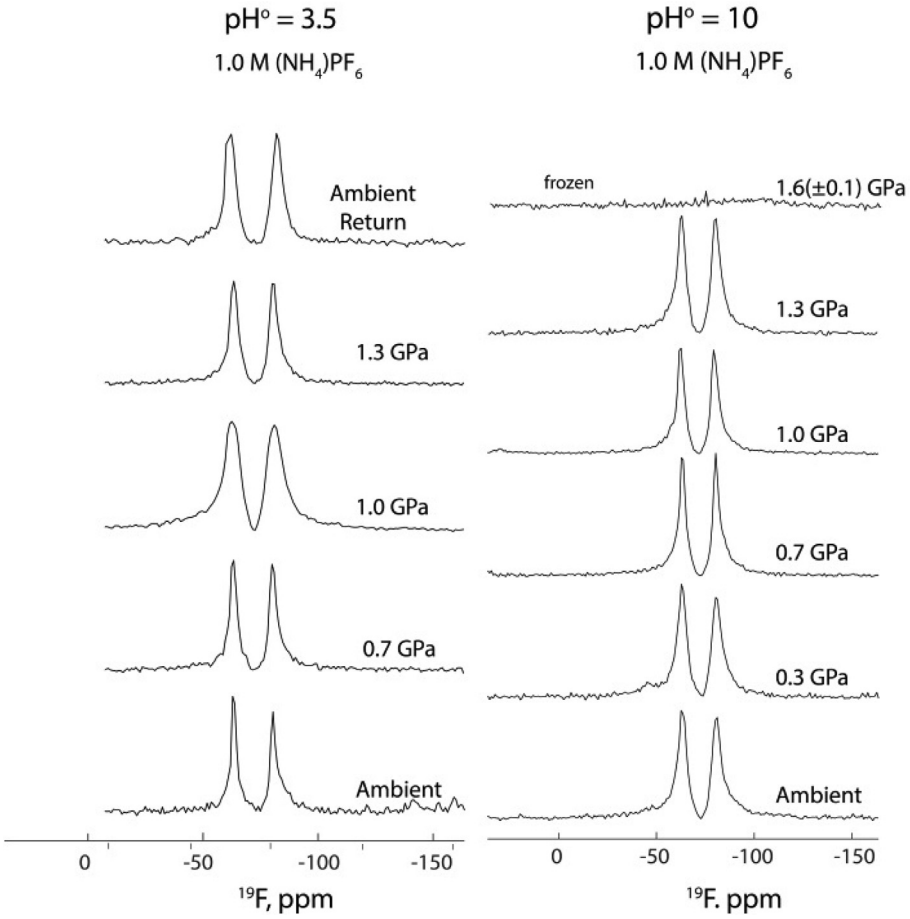


Fig. 1. $^{19}F$ spectra for 1.0 M $NH_4PF_6$ solution in $H_2O$. Spectra were collected as a function of pressure until the experimental solution froze at P > 1.3 GPa. After freezing, the pressure was returned to ambient and the spectra again indicated the $PF_6^-$(aq) ion in solution. The pressure uncertainty above ambient are ±0.1 GPa (one estimated standard deviation). Peak positions are assigned to be consistent with Fernandez-Galan et al. (1994).

raised beyond 1.3 GPa, which very likely indicates precipitation of a solid. An example is shown in Fig. 4. Increases in pressure cause the precipitation of the mineral Villiaumite and the reaction volumes could, in principle, be estimated using the NMR probe. The intensity of the peak assignable to the $BF_4^-$(aq) ion decreases at the highest pressure relative to the internal $PF_6^-$(aq) standard at most pH conditions (Supplemental Information, Figs. S-4 through S-6).

To test the precipitation hypothesis, we saturated a solution with NaF(s) at ambient conditions, where there is an excess of hydroxide ion (solution **1**), so that precipitation corresponds to a well-defined reaction:

$$4NaOH(aq) + BF_4^-(aq) = 4NaF(s) + B(OH)_4^-(aq) \quad (2)$$

The measured $^{19}F$ intensities of the peak assignable to the $BF_4^-$(aq) were normalized to the $PF_6^-$(aq) intensity standard and the ratios are shown in Fig. 5. The intensities suggest a pressure variation of this equilibrium constant:

$$K = \frac{[B(OH)_4^-]}{[NaOH]^4[BF_4^-]} \quad (3)$$

The loss of $^{19}F$ intensity at around −150 ppm indicates progress of the reaction to the right as written in Eq. (2) because the experiment was run at conditions where there is an excess of hydroxide.

### 3.3. $^{11}B$ NMR of fluoroborate species

The $^{11}B$ spectra for solutions **2** and **3** at ambient pressures (Fig. 6) show a distinct 1:3:3:1 quartet for the $BF_3OH^-$(aq) species and a singlet for the $BF_4^-$(aq) anion, consistent with the literature (Kuhlmann and Grant, 1964). The quartet arises from coupling between the $^{11}B$ (S = 3/2) nucleus and the $^{19}F$ (S = 1/2) nucleus ($J_{BF} \sim$ 15 Hz). Resolution is lost for solution **1** relative to the others because of the high ionic strength, and thus increased viscosity, of this solution relative to the others.

The high-pressure $^{11}B$ spectra for solution **2** (Fig. 7) exhibit three peaks that move and change in relative intensity with pressure. At ambient conditions in the high-pressure probe, a single broad peak is evident near 18 ppm that corresponds to aqueous borate species, specifically $B(OH)_3^0$(aq) and $B(OH)_4^-$(aq). Because the pH of the

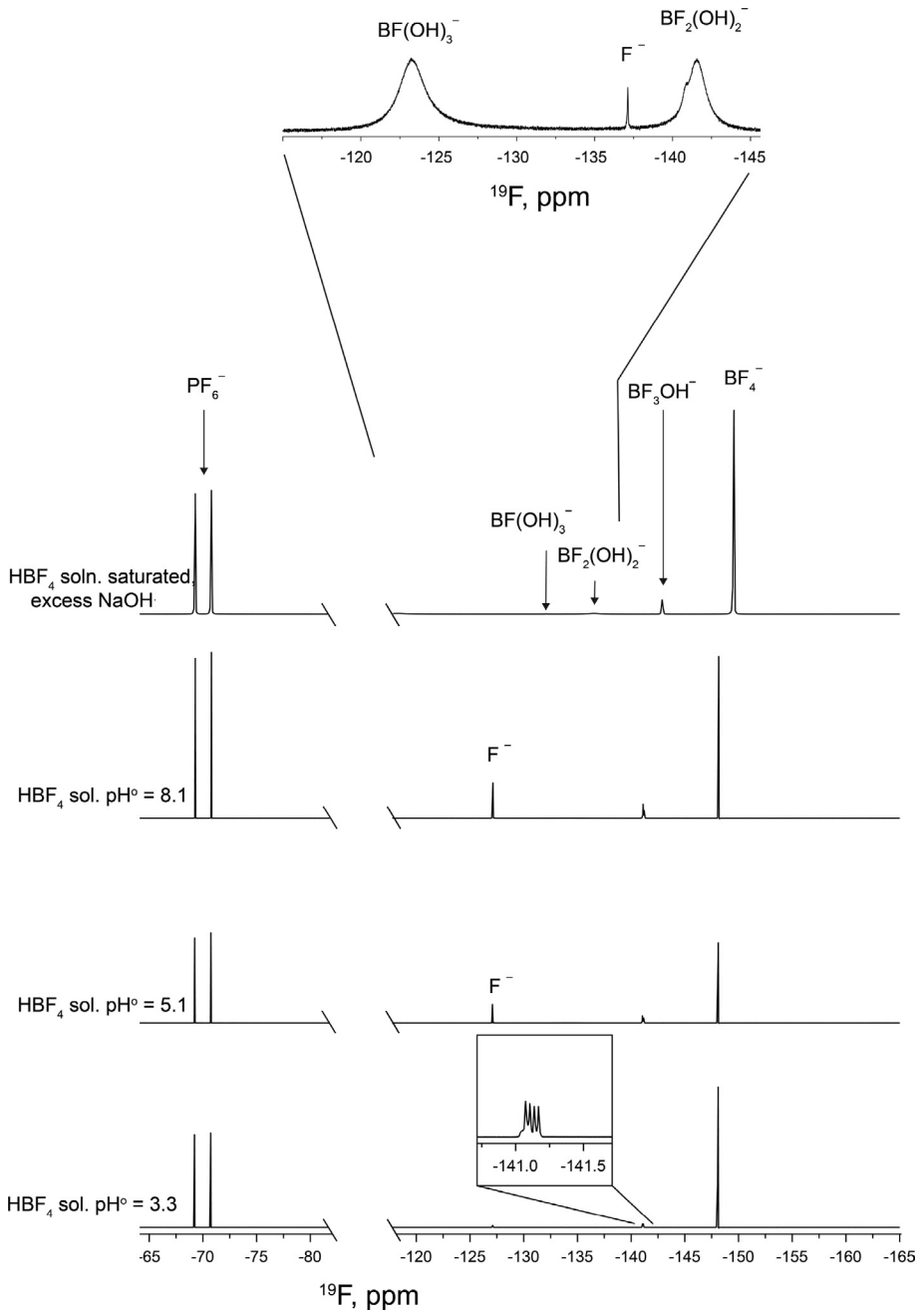


Fig. 2. $^{19}F$ spectra for solutions **1–4** at ambient pressure on a standard commercial NMR probe and spectrometer built around a superconducting magnet (11.7 T). Notice the $^{19}F$-$^{31}P$ $J_{FP}$-coupling of 742.7 Hz for the doublet assigned to the $PF_6^-$(aq) internal standard. The inset shows the 1:1:1:1 splitting ($J_{FB} = 14.5$ Hz) observed at −141 ppm in the $^{19}F$ spectra, which is consistent with coupling to $^{11}B$ (S = 3/2). The resolution diminishes with increased ionic strengths. The upfield chemical shift of the $BF_4^-$ and $BFOH_3^-$ signals relative to $PF_6^-$ for the solutions with excess NaOH are real.

sample (pH° = 8.1) is close to the $pK_a$ of boric acid (~9; Mesmer et al., 1973), the peak near 18 ppm includes contributions from both borate species. A single peak is observed because these species interconvert rapidly relative to the NMR timescale, with both the acid and conjugate base in near-equal concentrations, at least at ambient pressure.

Two other overlapping $^{11}B$ signals are evident in Fig. 7 near 0 ppm; these peaks are separated by only a few ppm. By comparison to Fig. 6, it is clear that these signals correspond to the $BF_4^-$(aq) and the $BF_3OH^-$(aq) ions. With increased pressure, these two peaks become unresolved, but the center of the composite peak moves downfield (to the left) so that the peak intensity is centered at 10 ppm at 1.3 GPa. The sample at this pressure failed catastrophically, so that the reversibility could not be demonstrated. However, almost all of the experimental solutions froze at

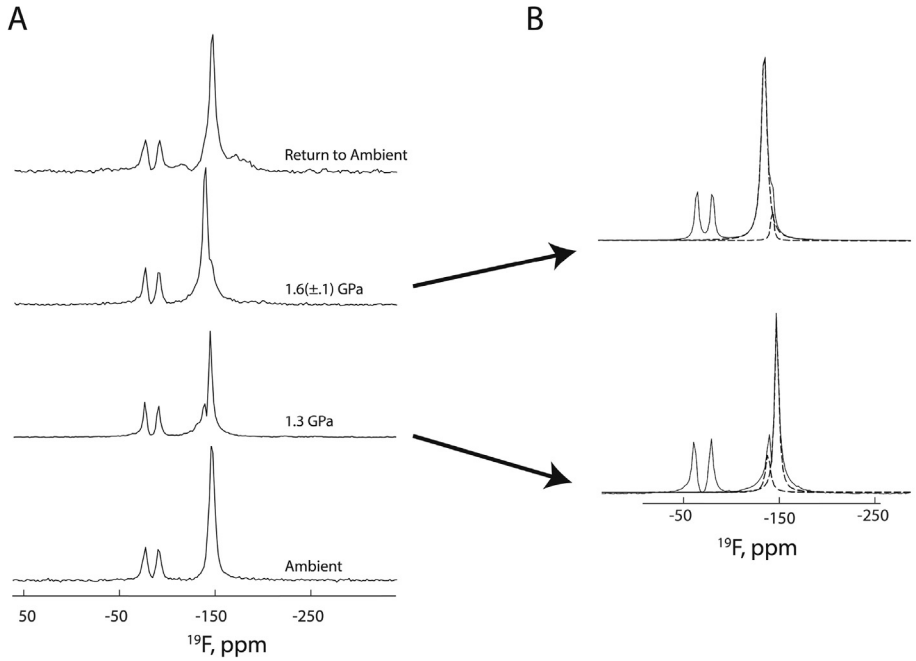


Fig. 3. (A) $^{19}$F spectra for solution **2** from ambient conditions to 1.6 GPa. The solution was compressed to freezing, then returned to ambient conditions in order to reproduce the original ambient spectra. The rest of the pressure series for solution **2** can be viewed in Fig. S-4. (B) The region of the spectra assigned to the $BF_4^-$(aq) and $BF_3OH^-$(aq) ions were fitted to Lorentzian shapes (dashed lines) and show two peaks that change in relative intensity with pressure.

pressures higher than 1.4 GPa and the ambient-condition signals return as pressure is relieved (Supplemental Information, Figs. S-4 through S-6).

## 4. DISCUSSION

There is comforting consistency between the $^{19}$F and $^{11}$B NMR spectra at pressure and the results are not surprising, save for two observations. First, $^{19}$F NMR signals for solution **2** seem to indicate reversible conversion of $BF_4^-$(aq) and $BF_3OH^-$(aq) at elevated pressure (Fig. 3). Second, there is some evidence for increased rates of $^{11}$B interconversion at elevated pressure. This evidence is the broadening and movement downfield for resonances assigned to the $BF_4^-$(aq) and $BF_3OH^-$(aq) signals (Fig. 7) into the signals assignable to the borate species, which are moving upfield (to the right). There are other potential causes of the observations, but these data suggest an area of fruitful future work, particularly given the sensitivity of boron reactions to pressure, as in the boron-diol reactions of Pautler et al. (2014).

One expects the peak positions of the boric acid/borate system to shift because the acid-base chemistry of both the solvent and solutes changes dramatically with pressure. The dissociation constant of water has a standard-state volume of reaction of $-22.3\ cm^3\ mol^{-1}$ such that it decreases by almost two log units at 298 K as pressure approaches 1.0 GPa (Marshall and Franck, 1981). Similar weak acids also dissociate more completely with pressure because of the increased dielectric constant of water (Fig. S-3, Supplemental Information). The $^{11}$B chemical shifts are particularly sensitive to the relative concentrations of boric acid and borate because the coordination number of boron increases from three to four upon dissociation. The $\Delta V°_{reaction}$ for trigonal boric acid to form tetrahedral borate is on the order of $-24\ cm^3$/mol because a bulk water is eliminated from solution as boric acid converts to borate (see Nalkina, 1983). Correspondingly, the $pK_a$ value drops by several units as pressure approaches 0.9 GPa. For samples with pH° near 8.1, the fraction of $^{11}$B in the conjugate base increases with pressure, causing the $^{11}$B resonance to shift upfield (to the right) and to become more narrow. This narrowing and movement upfield is evident in the signal that, at ambient pressures, lies near 18 ppm (Fig. 7).

Viscosity also increases with pressure and can increase linewidths, but not shift peak positions. Ochoa et al. (2016) showed for $LaCl_3$ and CsCl solutions, that viscosity might increase by a factor of 2–3 over this pressure range. However, the $^2$H signal from the $D_2O$ peak used for shimming did not broaden dramatically with pressure, as one would expect if viscosity alone were controlling the linewidths, which was surprising (see Supplemental Information, Fig. S-7).

This study was not intended to derive quantitative data about Villiaumite [NaF(s)] precipitation or fluoroborate equilibrium, but instead was intended to demonstrate new high-pressure NMR capabilities. Nevertheless, the variation in $^{19}$F intensities (Fig. 5) is consistent with a nonlinear change in the equilibrium constant with pressure. The solubility apparently rises initially at lower pressures and diminishes thereafter. The overall variation is on the order of a factor of five. A more detailed study could yield quantitative data about reaction volume as the $^{19}$F signals are complemented with $^{11}$B NMR spectra at pressure (see Reynolds and Belsher, 2017).

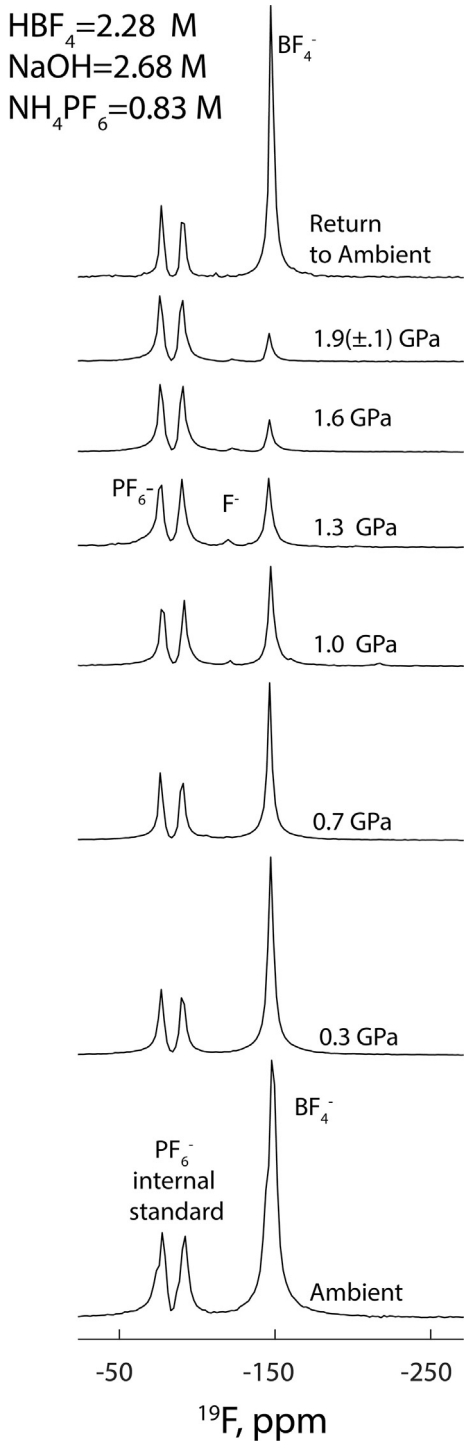


Fig. 4. Stacked spectra from a solution saturated with the mineral Villiaumite [NaF(s); solution **1**] from ambient pressure to 1.9 GPa. The small signal located between the $BF_4^-$(aq) and $PF_6^-$(aq) standard is free fluoride ion and there is excess NaOH in the solution. The estimated error in pressure is ±0.1 GPa.

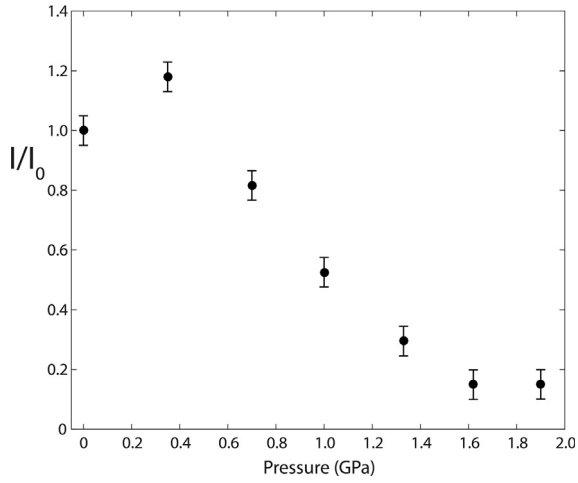


Fig. 5. Normalized intensity data for the saturated solution **1** from ambient pressure to 1.9 GPa. Signal intensity of the peak near −150 ppm (see Fig. 5) was normalized to the intensity standard by numerical integration at each pressure. The estimated error in pressure is ±0.03 GPa.

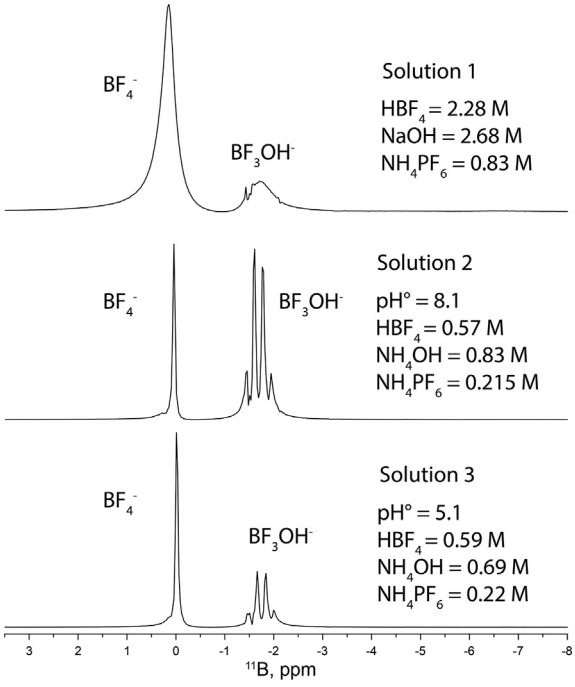


Fig. 6. $^{11}B$ spectra for solutions **1–3** collected at ambient pressure in the 300 MHz spectrometer. Coupling between $^{19}F$ and $^{11}B$ leads to a quintet of peaks in the $^{11}B$ spectrum for the $BF_4^-$(aq) ion, which cannot be resolved with the instrument, and a quartet for the $BF_3OH^-$(aq) ion. The ~15 Hz splitting due to J-coupling can be easily seen for the $BF_3OH^-$(aq) ion.

## 5. CONCLUSIONS

Solution NMR spectroscopy is possible on geochemically important aqueous solutions to gigapascal pressures and over a range of pH conditions. The experimental approach was adequate to demonstrate speciation changes in the fluoroborate system as gigapascal pressures where reached. Thus high-pressure NMR can complement other spectroscopies (e.g., Liu et al., 2012; Tooth et al., 2013;

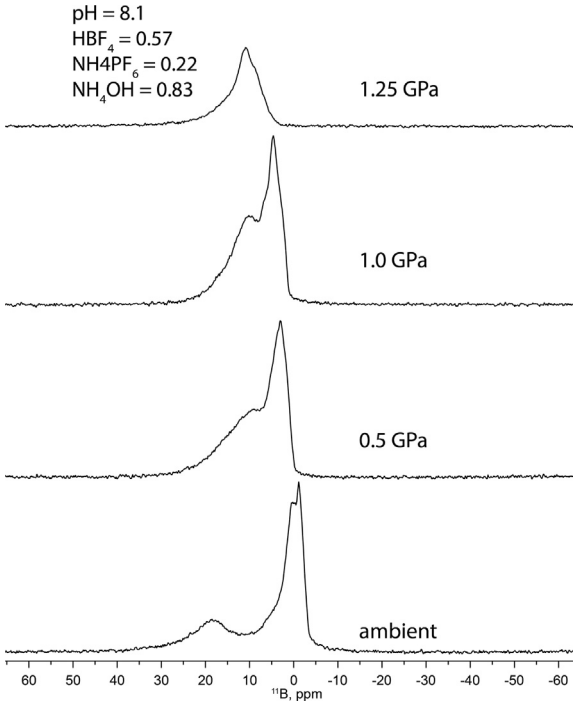


Fig. 7. $^{11}B$ spectra collected using the high-pressure probe for a solution similar in composition and age to **2**. At ambient pressures, the two peaks near 0 ppm correspond to the $BF_4^-$(aq) ion and the $BF_3OH^-$(aq) ion; here the $^{19}F$-$^{11}B$ splitting cannot be resolved. The broad peak near 18 ppm corresponds to $B(OH)_3^0$(aq) and $B(OH)_4^-$(aq) in rapid-exchange equilibrium. At this pH, the acid and conjugate base are nearly equal in concentration. However, the peaks broaden slightly and move upfield with increased pressure, until the signals partly coalesce with those assigned to the fluoroborate complexes. The sample failed at the highest pressure so that the ambient conditions could not be reproduced, as is typically done for other experiments.

Facq et al., 2016) and enrich the interpretation of solubility studies (e.g., Manning, 1994; Newton and Manning, 2000).

Some relatively straightforward technical issues must be overcome if collection of NMR spectra by aqueous geochemists at gigapascal pressures and high temperatures is to become routine. First, internal chemical-shift and intensity standards must also be identified that don't change position or decompose with pressure and temperature. The $PF_6^-$ ion that we use here could be employed for either $^{31}P$ or $^{19}F$ NMR, but other shift standards need to be found before chemical shifts can be interpreted to indicate pressure-induced changes in chemistry.

Secondly, a means of estimating pH at elevated pressures and temperatures *in situ* must be established. For ambient solutions there are several methods, such as the $^{31}P$ NMR peak positions of phosphate complexes (e.g., Yoza et al., 1994) or the $^{19}F$ peak position of fluoromolecules (Gerken, 2011), that could be adapted to hydrothermal conditions by careful experiments with phosphoric acid and $PF_6^-$.

Thirdly, hydrothermal experimentation requires that the common nonmagnetic alloys be replaced with new ones that retain strength at temperatures of a few hundred degrees Celsius and gigapascal pressures. Such alloys have recently been made available (Pascalloy™, Tevonic Corporation). Finally, adding temperature also requires alternative methods of measuring pressure *in situ* since the fluorescence of a ruby depends on temperature and pressure, but again these methods exist. The challenges are not insurmountable and it is possible that a well-accepted NMR shift thermometer, such $^1H$ NMR of aqueous ethylene glycol, can be adapted to provide a manometer as well.

If these difficulties can be overcome, then kinetic and thermodynamic data can be acquired at the molecular scale and at the conditions where the HKF model is employed for predictions of equilibrium constants. Species concentrations can be determined directly from spectra, as well as the rates of interconversion of molecules if the reactions proceed at the NMR timescale. Particularly sensitive to pressure, and ideal for study, are classes of reactions that have changes in solvation. These classes include aqueous metal systems where there is a change in coordination, such as the Si(IV), B(III), and Al(III) systems, and reactions that are enhanced by changes in the polarity or Brønsted acidity of the solvent. Silicon can easily change coordination from four to six by ligation to hydroxyl groups in certain sugars (Kinrade et al, 1999, 2001) and these are accompanied by large changes in $^{29}Si$ peak positions. Similarly, boric acid dissociates by adding a hydroxyl ion from water and thus changes coordination from three to four (Ishihara et al., 1994). Aluminum change coordination upon hydrolysis (e.g., Swaddle et al., 2005). Finally, changes in the solvent properties with pressure (the dielectric constant of water increases beyond 110 at low GPa pressures) suggests that some reactions could be catalyzed at pressure that are slow at ambient conditions.

## ACKNOWLEDGEMENTS

The authors particularly thank Associate Editor Catalano and three anonymous referee who provided criticisms that dramatically improved the manuscript. The authors also thank Peter Klavins and Dr. Jeff Walton for advice on probe design, and Dr. Dylan Sures for the viscosity measurements. This work is supported by the Office of Basic Energy Sciences, Chemical Sciences, Geosciences, and Biosciences Division via grant DE-FG02-05ER15693. The authors also thank Aspect Imaging for the magnet and spectrometer.

## APPENDIX A. SUPPLEMENTARY MATERIAL

Supplementary data to this article can be found online at https://doi.org/10.1016/j.gca.2018.09.033.

## REFERENCES

Amaya T., Wang W.-Z., Sakane H., Moriuchi T. and Hirao T. (2010) A dynamically inverting π-bowl complex. *Angew. Chem. Int. Ed.* **49**, 403–406.

Arunachalam M., Ahamed B. N. and Ghosh P. (2010) Binding of ammonium hexafluorophosphate and cation-induced isolation of unusual conformers of a hexapodal receptor. *Org. Lett.* **12**, 2742–2745.

Augustine M. P., Ochoa G. and Casey W. H. (2017) Steps to achieving high-resolution NMR spectroscopy on solutions at GPa pressure. *Am. J. Sci.* **317**, 846–860.

Baghurst D. R., Michael D., Mingos P. and Watson M. J. (1989) Application of microwave dielectric loss heating effects for the rapid and convenient synthesis of organometallic compounds. *J. Organomet. Chem.* **368**, C43–C45.

Ernst R. R. and Anderson W. A. (1966) Application of Fourier transform spectroscopy to magnetic resonance. *Rev. Sci. Instrum.* **37**, 93–102.

Facq S., Daniel I., Montagnac G., Cardon H. and Sverjensky D. A. (2016) Carbon speciation in saline solutions in equilibrium with aragonite at high pressure. *Chem. Geol.* **431**, 44–53.

Fernandez-Galan R., Manzano B. R., Otero A., Lanfranchi M. and Pellinghelli M. A. (1994) $^{19}F$ and $^{31}P$ NMR evidence for silver hexafluorophosphate hydrolysis in solution. New palladium difluorophosphate complexes and x-ray structure determination of [Pd(h-3-2-Me-$C_3H_4$)($PO_2F_2$)($PCy_3$)]. *Inorg. Chem.* **33**, 2309–2312.

Freire M. G., Neves C. M. S. S., Marrucho I. M., Coutinho J. A. P. and Fernandes A. M. (2010) Hydrolysis of tetrafluoroborate and hexafluorophosphate counter ions in imidazolium-based ionic liquids. *J. Phys. Chem. A* **114**, 3744–3749.

Gerken J. B. (2011) Measurement of pH by NMR spectroscopy in concentrated aqueous fluoride buffers. *J. Fluorine Chem.* **132**(1), 68–70.

Ishihara K., Nagasawa A., Umemoto K., Ito H. and Saito K. (1994) Kinetic study of boric acid-borate interchange in aqueous solution by $^{11}B$ NMR spectroscopy. *Inorg. Chem.* **33**, 3811–3816.

Kinrade S. D., Del Nin J. W., Schach A. S., Sloan T. A., Wilson K. L. and Knight C. T. G. (1999) Stable five- and six-coordinated silicate anions in aqueous solution. *Science* **285**, 1542–1545.

Kinrade S. D., Hamilton R. J., Schach A. S. and Knight C. T. G. (2001) Aqueous hypervalent silicon complexes with aliphatic sugar acids. *J. Chem. Soc., Dalton Trans.*, 961–963.

Kubas G. J., Monzyk B. and Crumblis A. L. (2007) Tetrakis (acetonitrile)copper(1+) hexafluorophosphate(1-). In *Inorganic Syntheses*. John Wiley & Sons, Inc., pp. 68–70.

Kuhlmann K. and Grant D. M. (1964) Spin-spin coupling in the tetrafluoroborate Ion 1a. *J. Phys. Chem.* **68**, 3208–3213.

Liu W., Migdisov A. and Williams-Jones A. (2012) The stability of aqueous nickel(II) chloride complexes in hydrothermal solutions: results of UV–Visible spectroscopic experiments. *Geochim. Cosmochim. Acta* **94**, 276–290.

Manning C. E. (1994) The solubility of quartz in $H_2O$ in the lower crust and upper mantle. *Geochim. Cosmochim. Acta* **58**, 4831–4839.

Marshall W. L. and Franck E. U. (1981) Ion product of water substance, 0–1000°C, 1–10,000 bars: new international formulation and its background. *J. Phys. Chem. Ref. Data* **10**, 295–304.

Meier T. (2018) Chapter One - at its extremes: NMR at giga-pascal pressures. In *Annual Reports on NMR Spectroscopy* (ed. G. A. Webb). Academic Press, pp. 1–74.

Meier T., Wang N., Mager D., Korvink J. G., Petitgirard S. and Dubrovinsky L. (2017) Magnetic flux tailoring through Lenz lenses for ultrasmall samples: a new pathway to high-pressure nuclear magnetic resonance. *Sci. Adv.* **3**, 5242.

Mesmer R. E., Palen K. M. and Baes C. F. (1973) Fluoroborate equilibrium in aqueous solutions. *Inorg. Chem.* **12**, 89–95.

Nalkina Z. A. (1983) The constant of dissociation of the boric acid at high pressures. *Izu. Sib. Otd. Akad. Nauk SSSR Ser. Khim. Nauk* **2**, 46–51.

Newton R. C. and Manning C. E. (2000) Quartz solubility in $H_2O$-NaCl and $H_2O$-$CO_2$ solutions at deep crust-upper mantle pressures and temperatures: 25 kbar and 500 C. *Geochim. Cosmochim. Acta* **64**, 2993–3005.

Ochoa G., Colla C. A., Klavins P., Augustine M. P. and Casey W. H. (2016) NMR spectroscopy of some electrolyte solutions to 1.9 GPa. *Geochim. Cosmochim. Acta* **193**, 66–74.

Ochoa G., Pilgrim C. D., Martin M. N., Colla C. A., Klavins P., Augustine M. P. and Casey W. H. (2015) $^{2}H$ and $^{139}La$ NMR spectroscopy in aqueous solutions at geochemical pressures. *Angew. Chem. Int. Ed.* **54**, 15444–15447.

Pautler B. G., Colla C. A., Johnson R. L., Klavins P., Harley S. J., Ohlin C. A., Sverjensky D. A., Walton J. W. and Casey W. H. (2014) A high-pressure NMR probe for aqueous geochemistry. *Angew. Chem. Int. Ed.* **53**, 9788–9791.

Reynolds J. G. and Belsher J. D. (2017) A review of sodium fluoride solubility in water. *J. Chem. Eng. Data* **62**, 1743–1748.

Sverjensky D. A., Harrison B. and Azzolini D. (2014) Water in the deep Earth: the dielectric constant and the solubilities of quartz and corundum to 60 kbars and 1200 °C. *Geochim. Cosmochim. Acta* **129**, 125–145.

Sverjensky D. A. and Huang F. (2015) Diamond formation due to a pH drop during fluid-rock interactions. *Nat. Commun.* **6**, 8702.

Swaddle T. W., Rosenqvist J., Yu P., Bylaska E., Phillips B. L. and Casey W. H. (2005) Kinetic evidence for five-coordination in $AlOH(aq)^{2+}$ ion. *Science* **308**, 1450–1453.

Tooth B., Etschmann B., Pokrovski G. S., Testemale D., Hazemann J.-L., Grundler P. V. and Brugger J. (2013) Bismuth speciation in hydrothermal fluids: An X-ray absorption spectroscopy and solubility study. *Geochim. Cosmochim. Acta* **101**, 156–172.

Wamser C. A. (1948) Hydrolysis of fluoboric acid in aqueous solution. *J. Am. Chem. Soc.* **70**, 1209–1215.

Yoza N., Ueda N. and Nakashima S. (1994) pH-dependence of $^{31}P$-NMR spectroscopic parameters of monofluorophosphate, phosphate, hypophosphate, phosphonate, phosphinate and their dimers and trimers Fresenius'. *J. Anal. Chem.* **348**(10), 633–638.

*Associate editor:* Jeffrey G. Catalano